Multimed Tools Appl (2017) 76:23957–23979
DOI 10.1007/s11042-016-4149-9

Amalgamation of iterative double automated thresholding and morphological filtering: a new proposition in the early detection of cerebral aneurysm

Abhijit Chandra[1] · **Sumita Mondal**[2]

Received: 28 January 2016 / Revised: 10 November 2016 / Accepted: 10 November 2016 /
Published online: 24 November 2016

Abstract Cerebral aneurysm (CA) has been emerging as one of the life threatening diseases in adults which results due to the pathological distension of cerebral arteries. Rupture of cerebral aneurysms causes subarachnoid hemorrhage (SAH) which is having a miserable prognosis. SAH is one of the cerebrovascular diseases with the highest mortality. With the rapid improvement in the field of medical image processing, prior detection of cerebral (intracranial) aneurysms before rupture is on a high rise. In this communication, we have made one novel attempt to detect CA from medical images through efficient amalgamation of automated thresholding and morphological filtering. In regard to this, an iterative double automated thresholding (IDAT) algorithm has been proposed which exhibits superiority over other existing thresholding techniques like Sauvola, Niblack and Otsu's threshold. Efficiency of the proposed algorithm has been validated over a number of digital subtraction angiography (DSA) images in terms of accuracy, sensitivity and specificity. The performance of the proposed method has also been compared with other existing methods for CA detection and finally its supremacy has been substantiated.

Keywords Cerebral aneurysm (CA) · Digital subtraction angiography (DSA) · Iterative double automated thresholding (IDAT) algorithm · Morphological filtering

✉ Abhijit Chandra
abhijit922@yahoo.co.in

Sumita Mondal
sumitam95@gmail.com

[1] Department of Instrumentation & Electronics Engineering, Jadavpur University, Sector III, Block LB, Plot No. 8, Salt Lake City, Salt Lake Bypass, Kolkata, West Bengal 700098, India

[2] School of Medical Science & Technology, Indian Institute of Technology, Kharagpur, India

1 Introduction

Cerebral aneurysm is most commonly formed at bifurcations on or near the base of the brain, known as Circle of Willis [16]. Persistent emplacement of aneurysms at arterial bifurcations suggests that the unique hemodynamics at bifurcation apices plays a key role in aneurysm formation. Subarachnoid hemorrhage (SAH) is considered to be a serious threat to patients in recent times which results due to ruptured intracranial aneurysm. SAH has a prevalence of sudden death of 12.4% and rates of casualty ranging from 32% to 67% after the hemorrhage [7]. A recent international study on un-ruptured cerebral aneurysms has found that the rupture rate of small (less than 5 mm diameter) aneurysms was only 0.05% per annum in patients with no prior SAH and 0.5% per annum for large (10 mm diameter) aneurysms [33].

However, majority of the un-ruptured aneurysms does not meet these criteria and it is difficult to predict the likelihood of their rupture. Un-ruptured small aneurysms are asymptotic while large aneurysms occasionally exhibit symptoms related to pressure on the adjacent brain or nerves. This pathological dilatation may be of congenital type or may develop with age. CA is generally named according to the artery or the segment of origin or both. In addition to single CA; multiple CA is also developed within human brain with an occurrence probability of 0.2 to 0.4.

Early detection of cerebral aneurysm has been receiving utmost importance amongst the medical practitioners of late. As a matter of fact, researchers throughout the globe have put their sincere efforts pertaining to the detection of CA at an early stage. A system for detecting CA automatically works with 3D X-ray rotational angiography (3DRA), computed tomography angiography (CTA) and magnetic resonance angiography (MRA) images using blob-enhancing filter [10]. Vascular geometry and identification of geometric features related to a specific pathological condition can throw sufficient light into the mechanisms involved in the pathogenesis of CA. There exists a complete framework for robust characterization of vascular geometry and its application in case of cerebral aneurysm [23]. Trivial techniques like dual thresholding along with smoothing filtering for extraction of region of interest in CA detection had been described in [18] in which morphological descriptors of aneurysms have been used to assess aneurysm rupture.

In this communication, we have made one novel attempt to detect CA of various sizes and multiplicity from 2D digital subtraction angiography (DSA) images. A detailed study of literature review suggests that DSA images are popularly employed as benchmark for successful detection of CA. As a major contribution of our proposition, a new double thresholding operation has been introduced for which upper and lower threshold values are selected in an iterative way. Impact of the proposed iterative double automated thresholding (IDAT) algorithm has been demonstrated over some of the existing thresholding techniques of recent interest with the help of a number of test images. One simple but elegant scheme has been proposed in this article which becomes capable in detecting CA from DSA images by means of an efficient amalgamation of the proposed IDAT algorithm and morphological filtering. In order to substantiate the impact of the proposed algorithm, fifteen such DSA images have been taken into our consideration and the resulting outcome has been presented accordingly. Efficiency of the proposed scheme over other existing algorithms has been quantitatively evaluated with respect to relevant performance indices like accuracy, sensitivity and specificity.

Entire paper has been organized as follows: Section 2 throws sufficient light on the existing algorithms which had become successful in detecting CA at an early stage. Section 3

establishes the novel proposition with the aid of mathematical background. Experimental results have been listed in Section 4, followed by the concluding remarks in Section 5.

2 Related works

CA is a cerebrovascular disorder which results from the localized bulging of blood vessels. In order to avoid rupture, pre-detection of CA is of utmost importance. As a matter of fact, research community throughout the globe has given major emphasis for accurate detection of CA with high sensitivity and specificity. Approaches of different researchers have added various dimensions to this problem. This section makes an honest effort in categorizing those different approaches into several groups on the basis of their similarity and works in each group have been presented in ascending chronological order.

2.1 Works pertaining to the identification of new features for CA detection

In order to indentify the possible occurrence of CA, the essential features have to be identified in the beginning. Zubillaga et al. [38] had correlated aneurysm neck size as an important feature for choosing proper treatment, while Ujiie et al. [28] introduced aspect ratio as a clinical measurement to predict aneurysm rupture. A basic immersed boundary (IB) method for the prediction of viscous flow in models for cerebral aneurysms had been shown in [17]. The gradient oscillatory number, a newly defined hemodynamic quantity, has been exploited as an index in [26] for CA initiation. Authors have also shown that this index is having a strong correlation with the location of aneurysm formation.

Potential of morphological descriptors had been explored by Valencia et al. [30] in which univariate and multivariate statistical analysis have identified that among the evaluated descriptors, Zernike moment invariants provided the best predictive capabilities of aneurysm rupture. In the year 2012, Hentschke and his co-workers have shown 13 new features which may be useful for the detection of CA with multi-modalities [11]. Morphological descriptors of aneurysms have also been used to assess aneurysm rupture. Study in [9] has revealed a new flow related parameter which can be used to predict aneurysm rupture.

2.2 Works pertaining to the prediction of CA

Prediction of CA has also been carried out by several researchers over a number of years. In connection to this, Brady and his research team have made predictions from hierarchical models for complex longitudinal data with application to aneurysm growth [4]. The idea that the natural history of un-ruptured intracranial aneurysms cannot be extrapolated from evaluation of patients with ruptured aneurysms is reinforced by the natural history data from the study of Wiebers [35]. These data also indicate that aneurysm size and location play a significant role in determining the risk of future rupture. A study in 2010 [24] has shown that there exists a correlation between intracranial aneurysm rupture with the ratio between aneurysm size and parent artery diameter.

The first probabilistic framework for a mechanically based rupture risk assessment of CA has been proposed in the year 2011 by Kroon [12]. In the same year, hemodynamic study [29] by Utami et al. has revealed the fact that wall shear stress is also playing a pivotal role in the initiation and development process of aneurysms. Wermer, on the other hand, suggests that

age, gender, population, size, site and type of the aneurysms should also be considered in the decision of treating an un-ruptured aneurysm [34]. Data mining techniques have been applied in [3] for predicting the rupture of cerebral aneurysms with 95% classification accuracy.

2.3 Works pertaining to the detection and classification of CA

A number of research articles are available in the literature which had introduced different algorithms for successful detection and classification of CA over the last few years. In regard to this, a diagnostic system based on visible spectroscopy has been developed on the basis of metabolite bilirubin leakage from a lumbar puncture to quickly and objectively assess low-blood volume SAH [2]. An automated classification method of CA from magnetic resonance angiography (MRA) images is proposed in [27] which had produced a new maximum intensity projection (MIP) images with the interested vessels only. This is carried out by manually selecting a cerebral artery from a list of cerebral arteries recognized automatically. A Bayesian classifier has been employed in [36] for the purpose of classifying CA from DSA images on the basis of geometry shape characteristics.

One semi automatic segmentation algorithm of intracranial aneurysms in CTA images had been developed in [21]. Output of the first phase is used by the radiologist to visually locate the aneurysm by selecting a point within the extent of the aneurysm which is subsequently used in the second phase to initialize the 3D level set algorithm in order to segment the complete aneurysm. Wang et al. proposed a method for segmenting giant aneurysms in CTA images using a multilevel object detection scheme which involves the use of lattice Boltzmann modelling [32].

A method for detecting CA by using 2D DSA imaging technique, based on the calculation of time to peak (TTP) and time duration (TD) of flow of contrast agent in the blood vessels has been developed in [37]. Cardenes and his co-researchers [6] had proposed one new automatic approach for isolating saccular intracranial aneurysms by neck detection using surface Voronoi diagram.

3 Methodology

This section explicitly describes the proposed algorithm for the efficient detection cerebral aneurysm of various sizes and multiplicity. In connection to this, an iterative double automated thresholding (IDAT) algorithm has been introduced and illustrated mathematically. Proposed IDAT algorithm together with some trivial image processing techniques has been successfully employed for the early detection of CA from DSA images.

3.1 Conversion of RGB image to grayscale image

Cerebral angiogram image has been employed in our approach which uses RGB color space. It has been converted into a grayscale intensity image (I) of size $N_R \times N_C$ where variables i and j represent position of pixel in horizontal and vertical direction respectively. This may be illustrated as:

$$I(i,j) = 0.299R(i,j) + 0.587G(i,j) + 0.114B(i,j) \;\forall\; \mathrm{i} \in \mathbb{I}_R \; and \; \mathrm{j} \in \mathbb{I}_C \tag{1}$$

$$with \; \mathbb{I}_R = 1, 2, \ldots\ldots\ldots, N_R \; and \; \mathbb{I}_C = 1, 2, \ldots\ldots\ldots, N_C,$$

where the coefficients R, G *and* B represent the perceptivity of human eye for red, green and blue color respectively. It converts the true color (RGB) image to grayscale intensity image by eliminating the hue and saturation information while retaining the luminance.

3.2 Image smoothing using Gaussian filter

Gaussian filter has been employed as a smoothing filter on the grayscale image which reduces image noise and retrieves the essential information. In general, linear smoothing filtering on the image (I) of size $N_R \times N_C$ with a filter (g) of mask size $m \times m$ can be expressed as:

$$F(i,j) = \sum_{a=-l}^{l} \sum_{b=-l}^{l} I(i+a, j+b) g(i,j) \quad where\ m = 2l+1, \quad with\ g(i,j) = \frac{1}{2\pi\sigma^2} e^{-\frac{i^2+j^2}{2\sigma^2}} \tag{2}$$

3.3 Thresholding

Identification and segmentation of major vessels and abnormal outgrowth of vessel wall from the background within the DSA image is executed by applying the thresholding operation. This section describes two types of thresholding operation, namely global binary thresholding and the proposed iterative double automated thresholding (IDAT) algorithm.

3.3.1 Global binary thresholding

Global binary thresholding is a technique which, when applied on the filtered image F, generates the image F_{GBT} consisting of extreme white and extreme black pixels only. For any threshold λ, gray values of the original image will be modified in accordance with the following equation:

$$F_{GBT}(i,j) = \begin{cases} 0 : \mathrm{F}(i,j) < \lambda \\ 1 : \mathrm{F}(i,j) \geq \lambda \end{cases} \tag{3}$$

3.3.2 Proposed iterative double automated thresholding (IDAT) algorithm

This article proposes a novel thresholding algorithm for the detection of CA from the DSA images. The proposed method is essentially a double thresholding technique in which lower and upper thresholds are calculated as governed by the following equations:

$$\lambda_L = \psi + \varphi \tag{4}$$

$$\lambda_U = \eta - \varphi \tag{5}$$

where the variables ψ, η *and* φ are calculated as:

$$\psi = \min_i \left[\min_j \{ F(i,j) \} \right] \forall\ i \in \mathbb{I}_R \ and\ \forall j \in \mathbb{I}_C \tag{6}$$

$$\eta = \max_i \left[\max_j \{F(i,j)\}\right] \forall\, i \in \mathbb{I}_R \text{ and } \forall\, j \in \mathbb{I}_C \tag{7}$$

$$\varphi = \frac{\psi + \eta}{2} \tag{8}$$

Depending upon the values of lower and upper threshold, a new image F_{AT} is formed as outlined below:

$$F_{AT}(i,j) = \begin{cases} 0 : \mathrm{F}(i,j) < \lambda_L \\ 1 : \mathrm{F}(i,j) \geq \lambda_U \end{cases} \tag{9}$$

It can be explicitly seen from Eq. (9) that the image F_{AT} is not completely binary as it contains few gray pixels within the range [λ_U λ_L]. A 3 × 3 window centered around the pixel (i, j) is therefore placed for all such image pixels $F(i,j)$ which belong to the range $\lambda_U < F(i,j) < \lambda_L$. Central pixel under this mask is subsequently replaced by a new variable σ which is calculated in accordance with Eq. (10):

$$\sigma = \left[\sum_{\substack{b=-1 \\ b \neq 0}}^{1} \sum_{a=-1}^{1} F(i+a, j+b) \right] + F(i-1, \mathrm{j}) + F(i+1, \mathrm{j}) \tag{10}$$

With the introduction of the variable σ, other relevant variables pertaining to the algorithm are calculated as:

$$\psi_\sigma = min_{i_\sigma} \left[min_{j_\sigma} \{F(i, \mathrm{j})\} \right] \forall i_\sigma \in \mathbb{I}_{R_\sigma} \; and \; \forall\, j_\sigma \in \mathbb{I}_{C_\sigma} \tag{11}$$

$$\eta_\sigma = max_{i_\sigma} \left[max_{j_\sigma} \{F(i, \mathrm{j})\} \right] \forall i_\sigma \in \mathbb{I}_{R_\sigma} \; and \; \forall\, j_\sigma \in \mathbb{I}_{C_\sigma} \tag{12}$$

$$\varphi_\sigma = \frac{\psi_\sigma + \eta_\sigma}{2} \tag{13}$$

$$\lambda_{L_\sigma} = \psi_\sigma + \varphi_\sigma \tag{14}$$

$$\lambda_{U_\sigma} = \eta_\sigma - \varphi_\sigma, \tag{15}$$

where the presence of subscript σ identifies that the central pixel of the set is modified by σ.

With the replacement of central pixel by the variable σ, new lower and upper threshold values are utilized to categorize the previous gray pixels in any of the two binary classes. This may be mathematically formulated as:

$$F_{AT_\sigma}(i,j) = \begin{cases} 0 : \mathrm{F}(i,j) < \lambda_{L_\sigma} \\ 1 : \mathrm{F}(i,j) \geq \lambda_{U_\sigma} \end{cases} \tag{16}$$

This iterative process continues until all the gray pixels are taken into consideration and it consequently converts the grayscale image into a binary one. Since the proposed algorithm

considers the operation of double thresholding in an iterative way; it is termed as iterative double automated thresholding (IDAT) algorithm.

3.4 Morphological filtering

Extraction of the vessel outgrowth is carried out by applying morphological filtering on the binary image obtained through thresholding operation. This filter performs two consecutive operations, namely opening followed by closing morphology. Opening and closing help to decrease the size of the small bright and dark details from an image respectively. Operations like opening and closing are composed of two fundamental morphological techniques, called dilation and erosion.

Although opening and closing are considered generic image processing techniques, impact of this morphological filtering in any particular application is generally governed by the sequence of operation and the nature and size of the structuring element. This issue has been dealt with justified attention in our analysis. CA images are generally seen as an interconnected topology of abnormal outgrowth of blood vessels. Objective of CA detection lies in identifying those abnormalities from the brain image. As the connecting blood vessels carry almost no significance about the occurrence and type of the aneurysm; they are initially made thinner by virtue of opening operation. This leads to the removal of thin protrusions and breaking of narrow joins. Subsequent closing operation compensates the loss due to opening in the aneurysm-affected area and eventually reverts back its original shape without the presence of blood vessels. It can be clearly observed from DSA images that the expansion of aneurysm-affected area is more than the normal blood vessels. As a matter of fact, proposed method of employing opening operation followed by closing morphology is proved to be useful. Since the outgrowth of blood vessels generally takes place uniformly, structuring element with symmetricity in horizontal, vertical and diagonal direction has been selected in this particular experiment. Mathematical illustration of these techniques is briefly presented below:

The set of Euclidean coordinates corresponding to the input binary image F_{AT_σ} eroded with the structuring element D is given by:

$$F_{AT_\sigma} \ominus D = \{w : D_w \subseteq F_{AT_\sigma}\}, \tag{17}$$

where D_w signifies translation of D at its origin w, i.e. for any $w = (x, y)$, $D_w = \{(a, b) + (x, y) : (a, b) \in D\}$.

The set of Euclidean coordinates corresponding to the input binary image F_{AT_σ} dilated with structuring element D can be outlined as:

$$F_{AT_\sigma} \oplus \mathrm{D} = \underset{w \in D}{\cup} F_{AT_{\sigma_w}} \tag{18}$$

These two fundamental morphological operations are employed to construct higher order techniques like opening and closing. For the image F_{AT_σ} and the structuring element D, opening of F_{AT_σ} by D is given by:

$$F_{AT_\sigma} \circ D = (F_{AT_\sigma} \ominus D) \oplus D = \cup\{D_w : D_w \subseteq F_{AT_\sigma}\} \tag{19}$$

Closing operation, on the other hand, employs the same two fundamental operations in a reverse order. For the same input image and structuring element, closing is mathematically represented as:

$$F_{AT_\sigma} \cdot D = (F_{AT_\sigma} \oplus D) \ominus D = \left\{ w : D_w \subseteq \bigcup_{w \in D} F_{AT_{\sigma_w}} \right\} \tag{20}$$

In order to eliminate the thin protrusions and segregate the vessel outgrowth from the DSA image, opening and closing operations have been applied on the binary image F_{AT_σ} obtained through IDAT algorithm. Resultant image F_{MF} may be represented as:

$$F_{MF} = \{(F_{AT_\sigma} \circ D) \cdot D\} \tag{21}$$

where the symbols $\circ$ and $\cdot$ signify opening and closing operations respectively.

3.5 Edge detection

Edge detection is the process of localizing the pixel intensity transitions. Edge detection of the vessel outgrowth in DSA image is carried out by applying the Sobel mask Δ of size $(2k+1) \times (2k+1)$ on F_{MF} which yields the image F_S in accordance with the following equation:

$$F_S(i, \mathrm{j}) = \sum_{s=-k}^{k} \sum_{t=-k}^{k} F_{MF}(i+s, \mathrm{j}+t).\Delta(s,t) \tag{22}$$

Edge detected image F_S is finally superimposed on the original DSA gray image and the affected area is marked accordingly. Proposed algorithm for the early detection of cerebral aneurysm has been summarized by means of a flow chart as shown in Fig. 1 below.

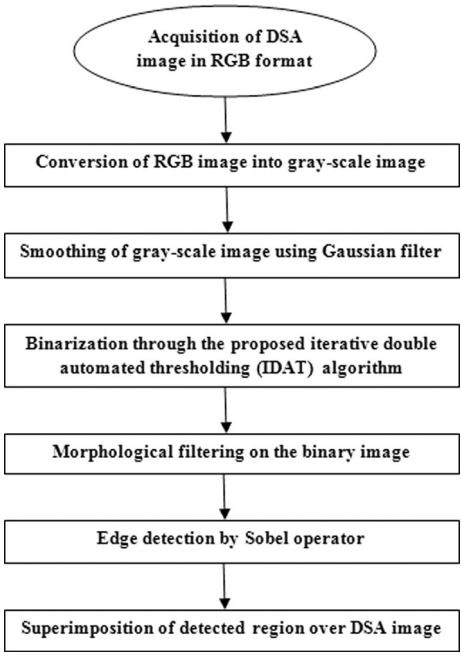

Fig. 1 Flowchart of the proposed algorithm for the detection of CA from DSA image

4 Simulation results

Competence of the proposed algorithm in detecting CA of various sizes and multiplicity has been substantiated with the help of fifteen DSA test images. These test images are obtained from the yardstick database of Dr. Balaji Anvekar's Neuroradiology Cases [8] and Brain Aneurysms Foundations [5]. In regard to this, supremacy of the proposed IDAT algorithm has been demonstrated by selecting five test images from the set because of the space constraint and the resultant performance has also been compared with three most widely cited thresholding algorithms, i.e., local binarization techniques of Sauvola [25], Niblack [20] and the global thresholding of Otsu [22] in Figs. 2, 3, 4, 5 and 6 below. The set of these test images is selected in such a way that it can faithfully embed all such possible abnormalities due to CA in human brain and hence can perform a robust comparative analysis with other existing algorithms pertaining to the detection of CA. The entire set of DSA test images has been classified in terms of their size and multiplicity as listed in Table 1 below.

Detection of CA from these DSA images has further been demonstrated in Figs. 7, 8, 9, 10 and 11 in which the impact of several image processing techniques towards the fulfillment of the objective has been explicitly elaborated. More specifically, original DSA and grayscale image have been shown in part (a) and (b) of each figure respectively. Resulting images after subsequent application of Gaussian filter followed by IDAT algorithm have serially been depicted in part (c) and (d) respectively. Impact of morphological operations in extracting the aneurysm-affected region has been described in part (e), followed by the edge detection by Sobel operator in part (f). Finally, the detected area is superimposed on the original DSA image in part (g) of each figure. Entire simulation has been carried out using MATLAB 7.10.0 software.

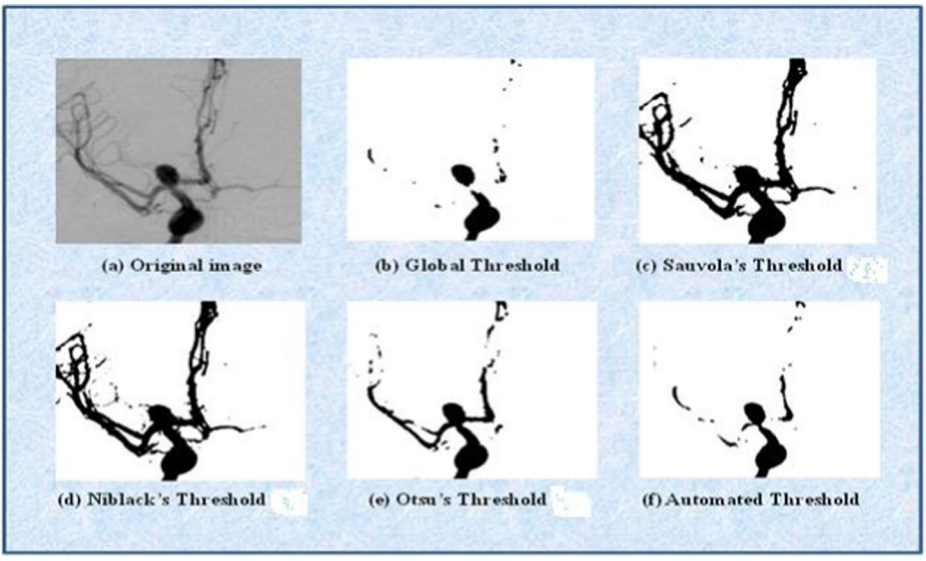

Fig. 2 Performance comparison with test image 1

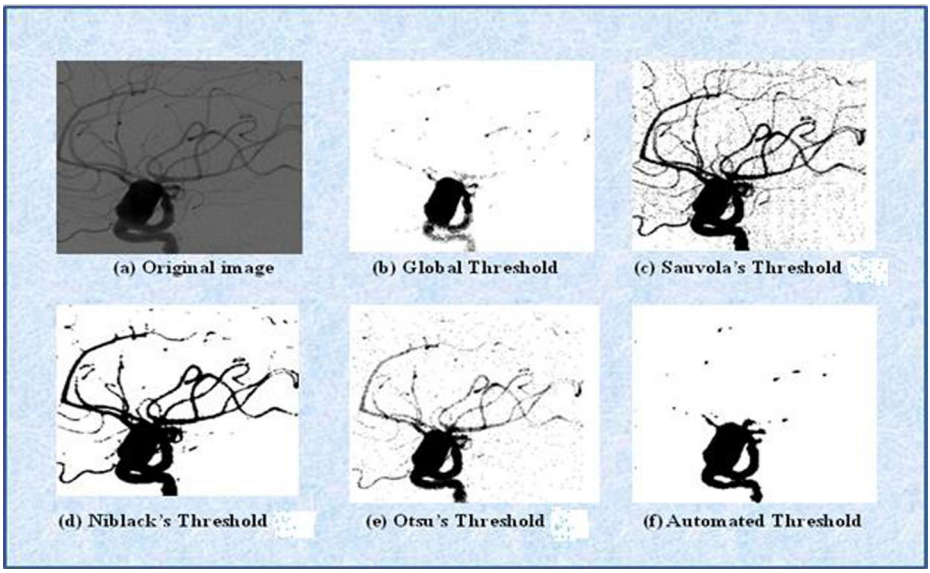

Fig. 3 Performance comparison with test image 2

It can be unambiguously observed from the above figures that automated thresholding algorithm together with the morphological filtering eliminates majority of the blood vessels while retaining the complete aneurysm portion. Performances of other existing thresholding algorithms are quite inferior to the proposed method in the sense that they contain a significant amount of blood vessels even after binarization. Figures 7, 8, 9, 10 and 11 ascertains the

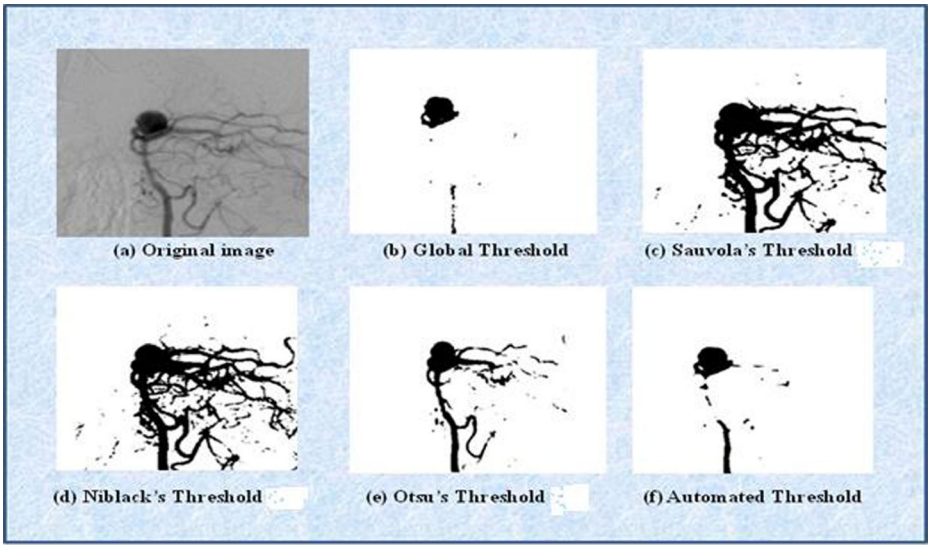

Fig. 4 Performance comparison with test image 3

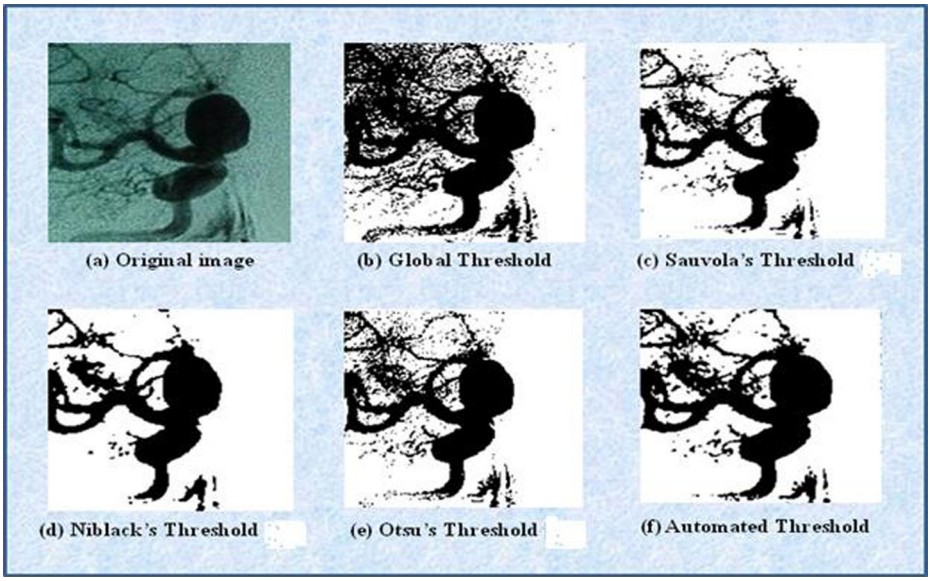

Fig. 5 Performance comparison with test image 4

impact of morphological filtering in extracting the aneurysm-affected area from these binary images obtained through proposed IDAT algorithm. In addition to these five test images, ten more DSA images have been taken into our consideration for the purpose of substantiating the robustness of the proposed detection algorithm. Our observations with these images have been reported in Figs. 12, 13, 14, 15, 16, 17, 18, 19, 20 and 21

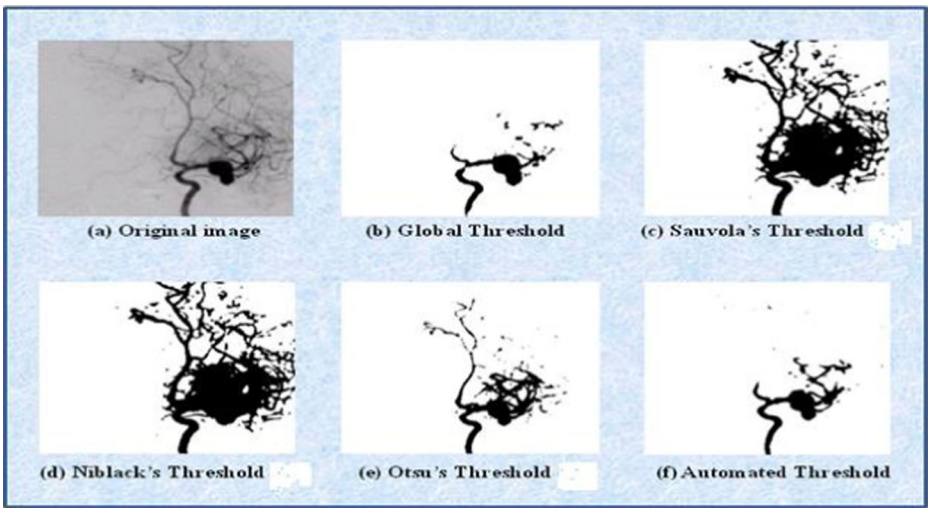

Fig. 6: Performance comparison with test image 5

Table 1 Classification of DSA test images

Type		Image number
Size	Small	5, 7, 11
	Medium	1, 3, 9, 10, 12, 14
	Large	2, 4, 6, 8, 13, 15
Multiplicity	Single	2, 3, 5, 6, 7, 8, 9, 12, 13, 15
	Multiple	1, 4, 10, 11, 14

below. It has also been proved that the proposed scheme of amalgamation between IDAT algorithm and morphological filtering is successful in detecting CA from two-dimensional DSA images of various types.

Table 1 clearly reflects that the test images considered in Figs. 12, 13, 14, 15, 16, 17, 18, 19, 20 and 21 possess sufficient versatility in terms of size and multiplicity. This set includes different types of aneurysms like small single (image 7), small multiple (image 11), medium single (images 9, 12), medium multiple (image 14), large single (images 13, 15) and so on. Experimental observations in the above figures undoubtedly reveal that the proposed algorithm becomes competent in identifying CA by eliminating the blood vessels and other unnecessary portions from the DSA image. This has been obtained after applying morphological filtering on the binary image as shown in part (d) of each of these figures. Detected area has subsequently been identified on the original image with the help of an edge marked with red color and been represented in part (e). Detected area has finally been superimposed on the DSA image in the last part of each of these figures.

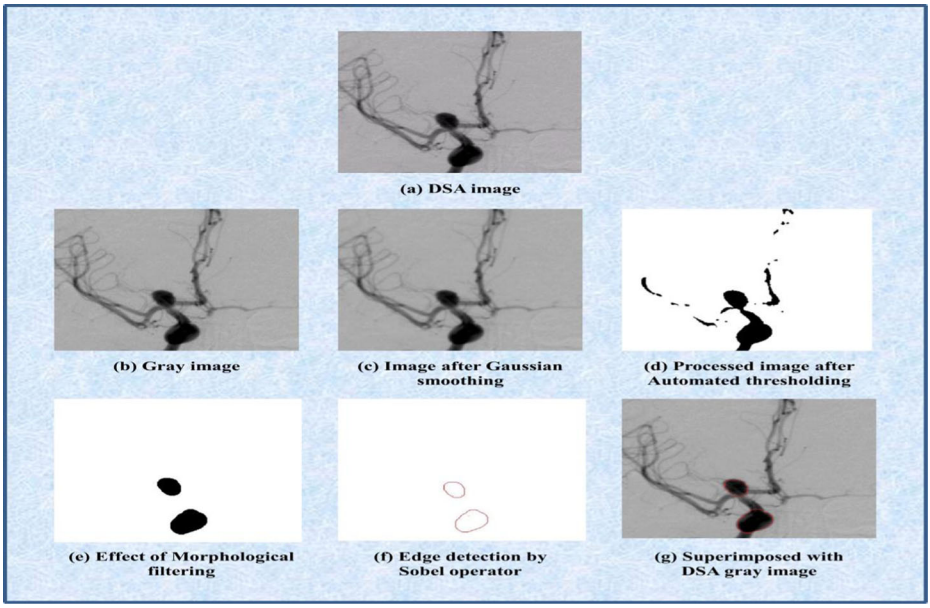

Fig. 7 Detection of CA from test image 1

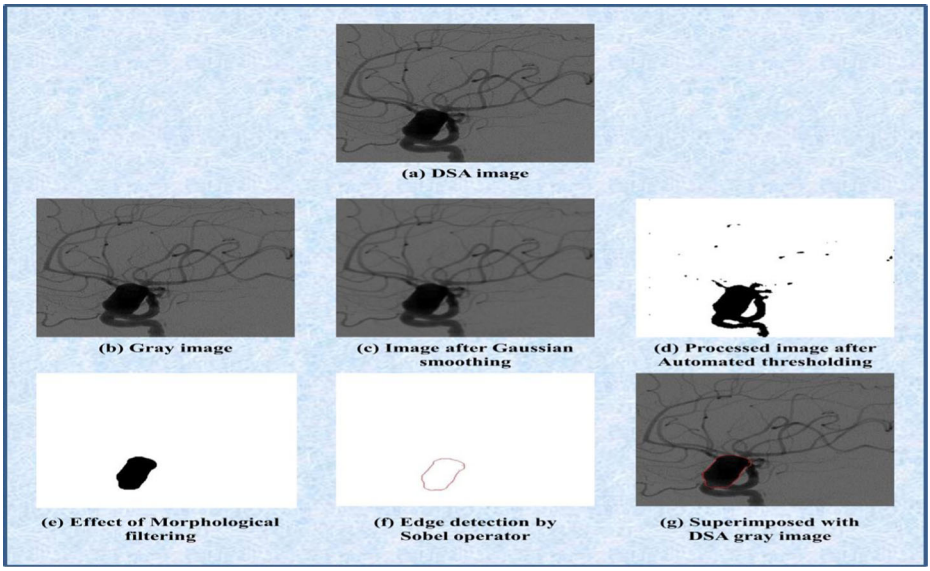

Fig. 8 Detection of CA from test image 2

Experimental results in the above figures qualitatively demonstrate the efficiency of the proposed scheme in detecting CA from the DSA images. In addition to this, images generated by the proposed algorithm have subsequently been compared with the manually detected images by means of relevant performance parameters. These parameters, namely Accuracy ($\mathcal{A}$), Sensitivity ($\mathcal{S}$) and Specificity (&) have been defined as follows [1, 14]:

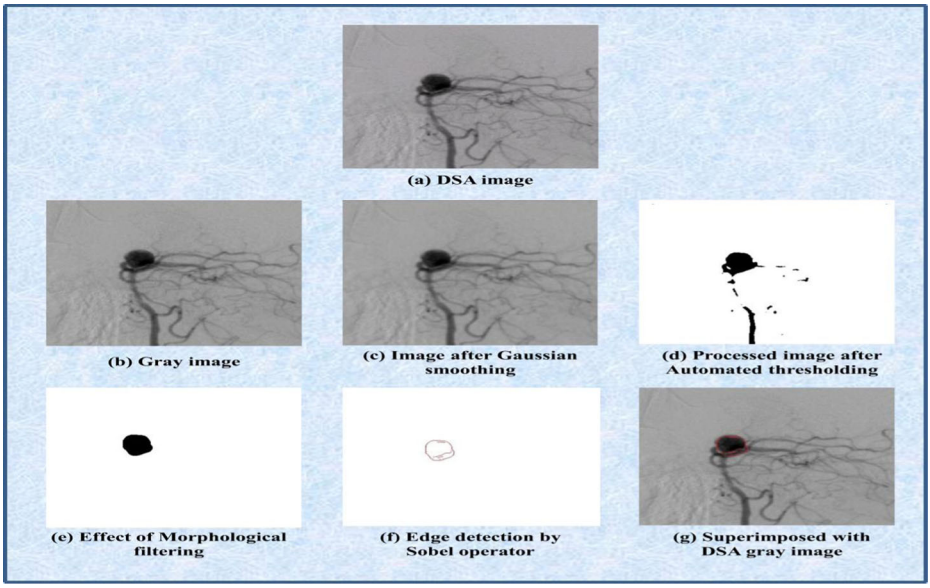

Fig. 9 Detection of CA from test image 3

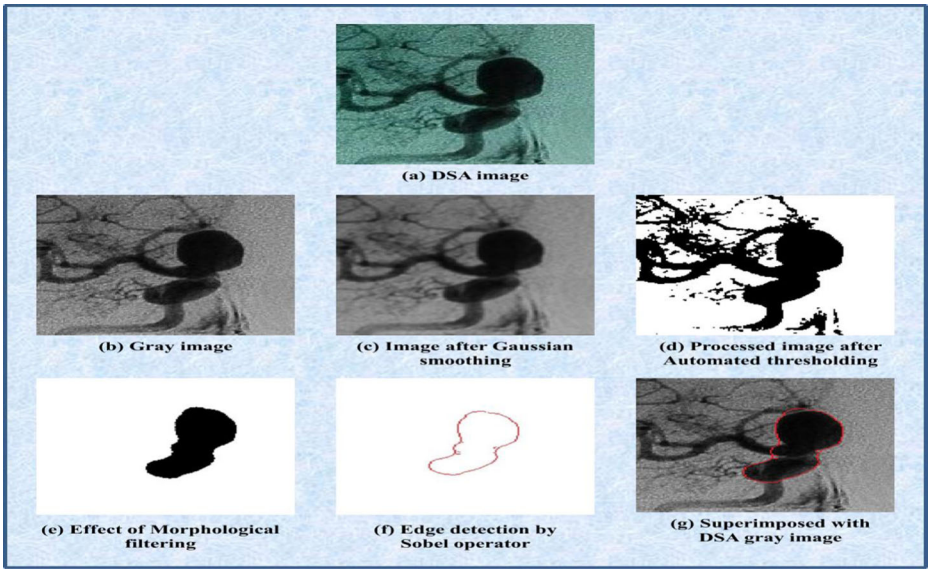

Fig. 10 Detection of CA from test image 4

$$\mathcal{A} = \left(1 - \frac{\alpha - \beta}{\beta}\right) \times 100\% \tag{23}$$

where α represents the computed segmented area in pixels using the proposed algorithm and β is the ground truth.

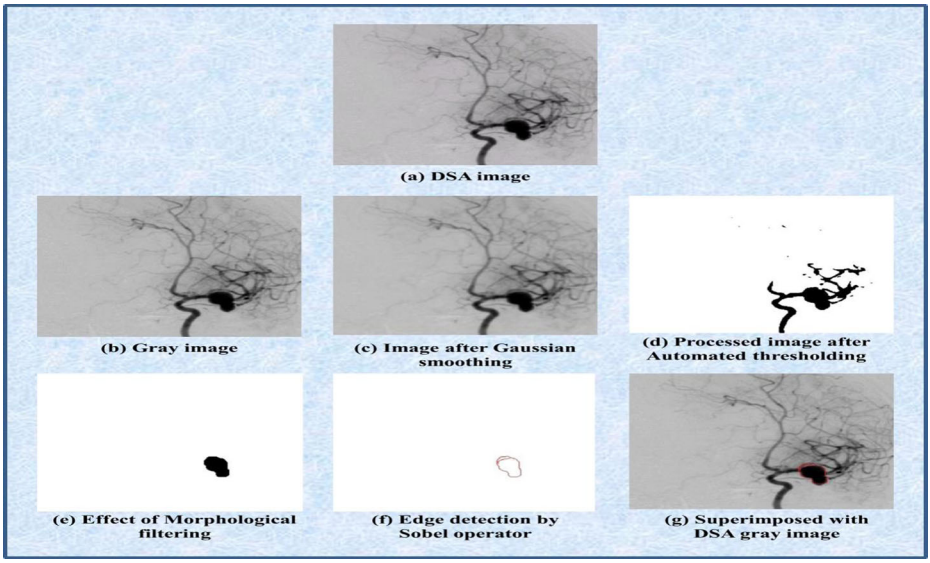

Fig. 11 Detection of CA from test image 5

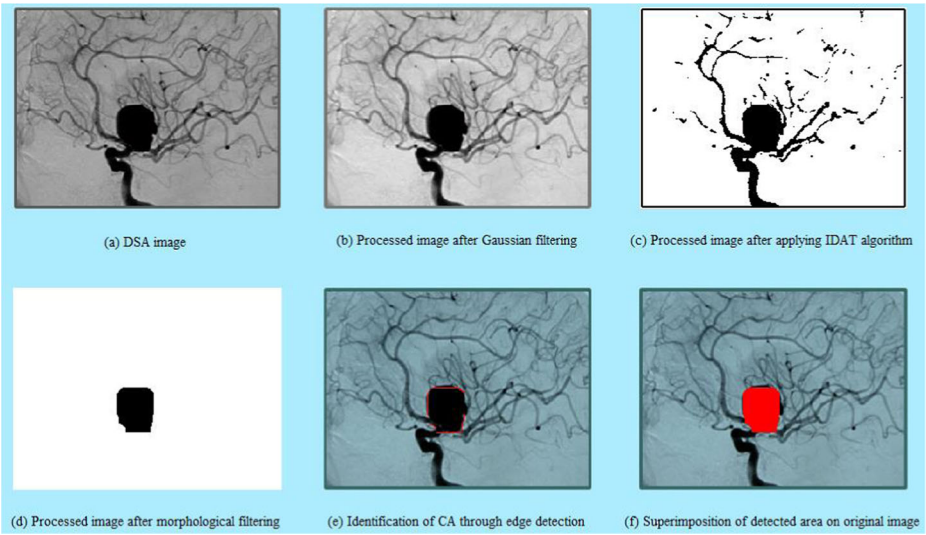

Fig. 12 Detection of CA from test image 6

$$\mathcal{S} = \frac{\text{True Positive}}{\text{True Positive} + \text{False Negative}} \tag{24}$$

where *True Positive* is considered as correctly identified and *False Negative* is equivalent to incorrectly rejected.

$$\& = \frac{\text{True Negative}}{\text{True Negative} + \text{False Positive}} \tag{25}$$

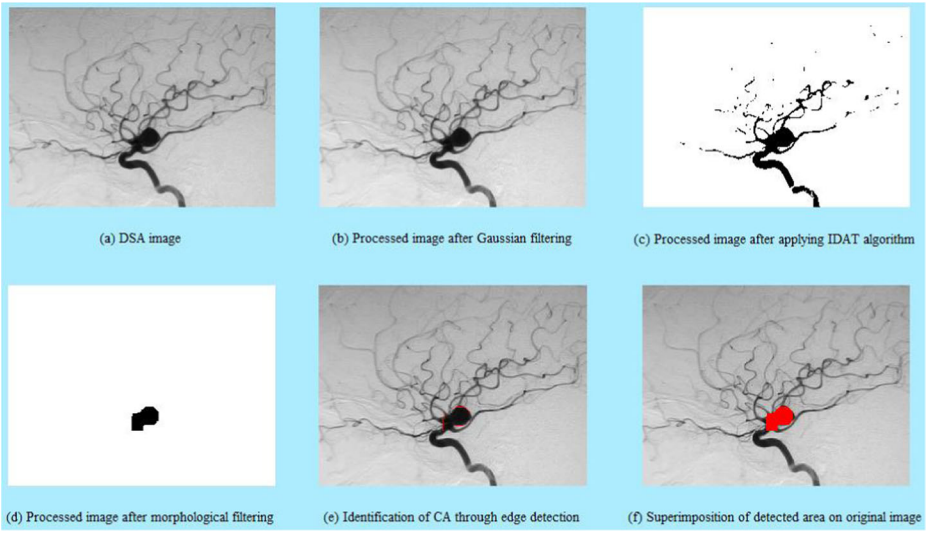

Fig. 13 Detection of CA from test image 7

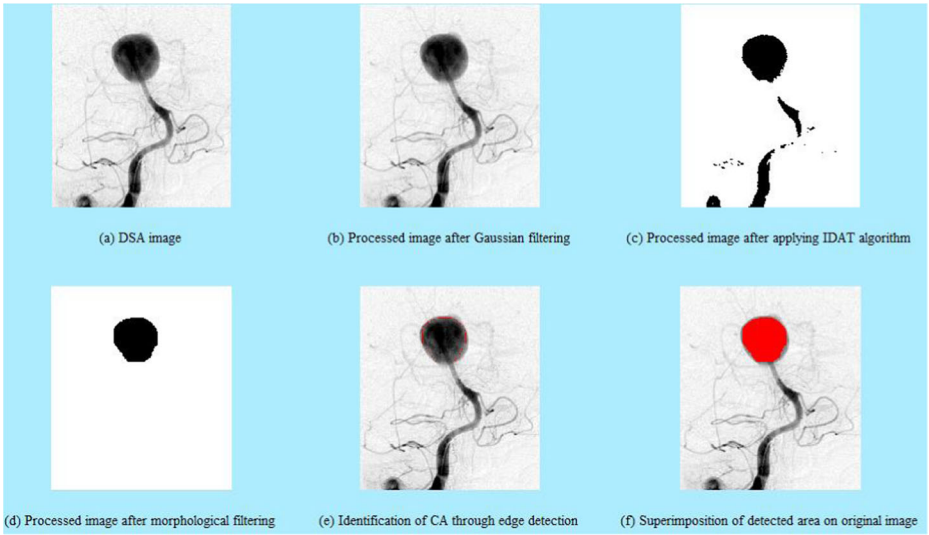

Fig. 14 Detection of CA from test image 8

where *True Negative* is treated as correctly rejected and *False Positive* is incorrectly identified.

In order to examine the effectiveness of the proposed approach, manual detection of each of the test images has been separately carried out and subsequently compared with the results of automatic detection. Resultant performance of our proposition in detecting CA from the DSA images has been evaluated in terms of accuracy, sensitivity and specificity for all the fifteen test images considered in this analysis. Supremacy of the proposed scheme has finally been established by making a comparative study with other existing techniques for the detection of CA in terms of these performance indices and our observations have been summarized in Table 2 below.

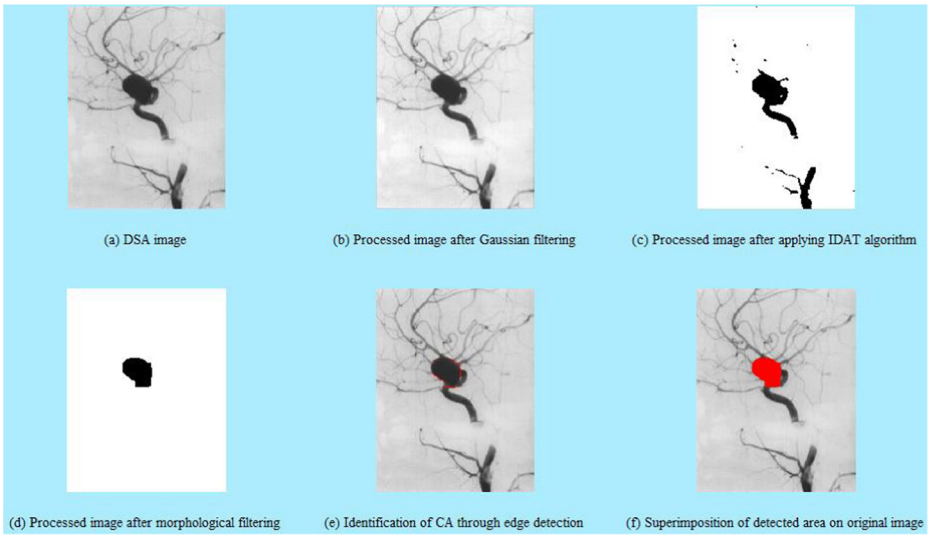

Fig. 15 Detection of CA from test image 9

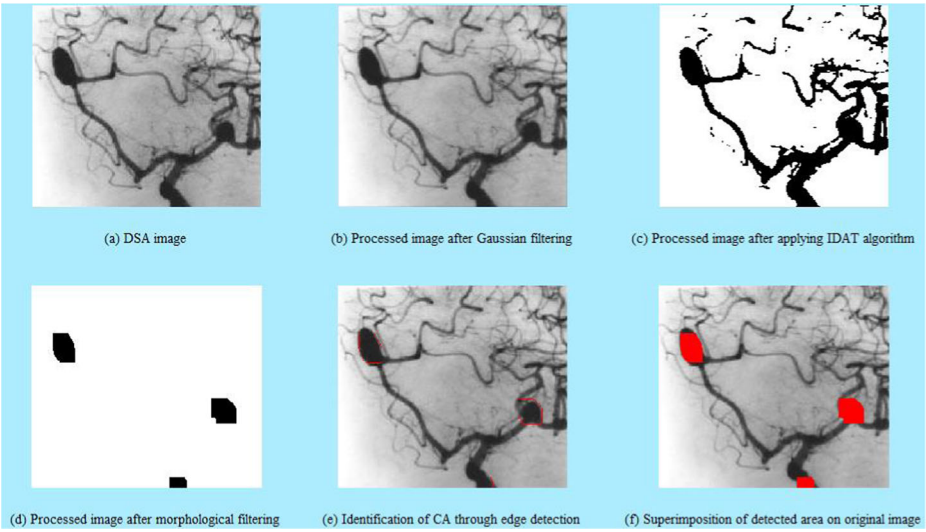

Fig. 16 Detection of CA from test image 10

Looking at the entries at Table 2, it can be well apprehended that the amalgamation of IDAT and morphological filtering performs reasonably well towards the early detection of CA with a higher degree of accuracy. Except for two test images (images 8 and 10), resultant accuracy reaches around 98–99% which is clinically acceptable to the medical practitioners. Moreover, as far as the values of sensitivity and specificity are concerned, proposed algorithm minimizes the possibility of false detection (false positive) and missed detection (false negative) to a significant extent. Average performance of all the images clearly identifies that IDAT algorithm together with morphological filtering produces

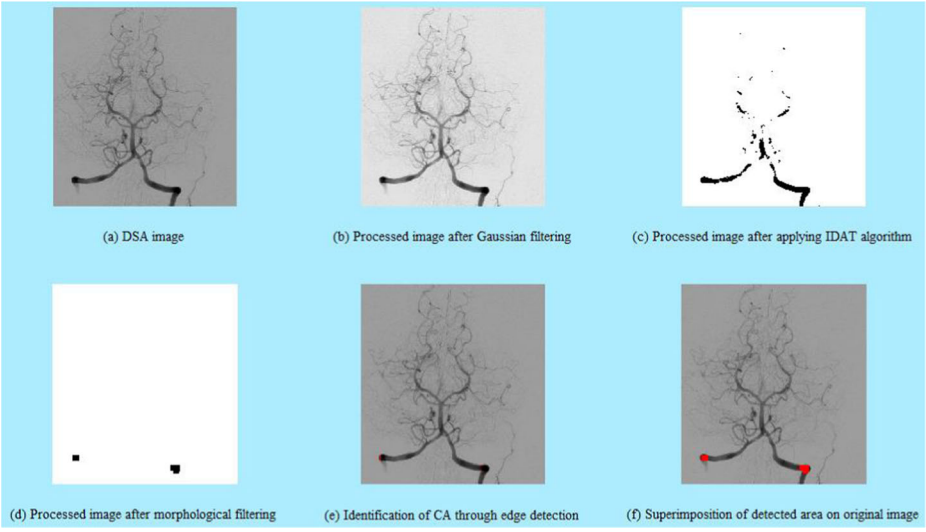

Fig. 17 Detection of CA from test image 11

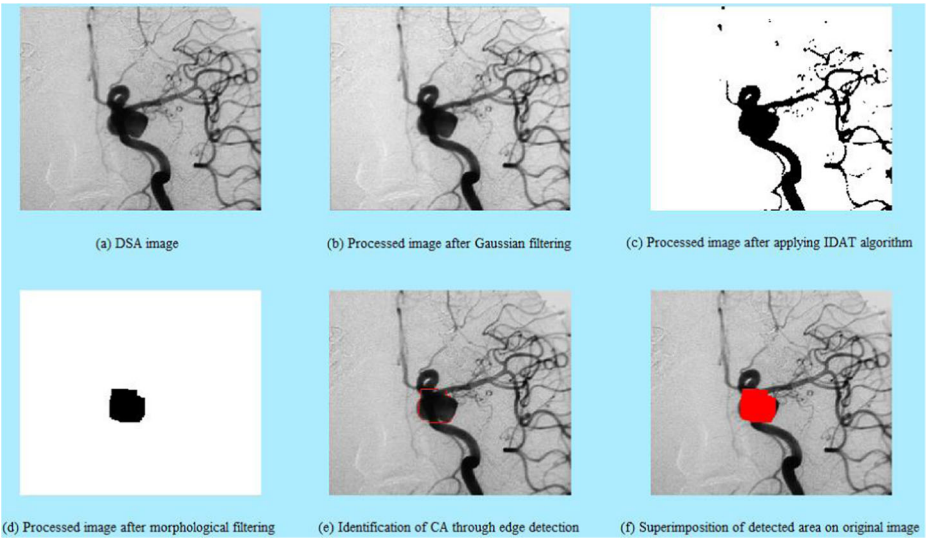

Fig. 18 Detection of CA from test image 12

better or comparable result than the existing articles in the literature. As a matter of fact, proposed algorithm projects itself as a viable tool for the early detection of CA from DSA images with varying size and multiplicity.

5 Conclusion

This paper introduces one novel scheme for the automatic and successful detection of CA from DSA images. A new double thresholding algorithm has been proposed in this context which

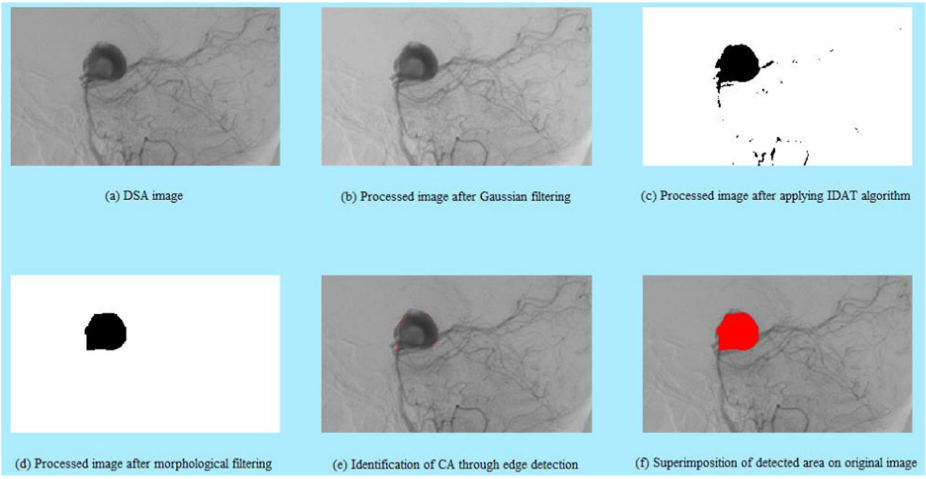

Fig. 19 Detection of CA from test image 13

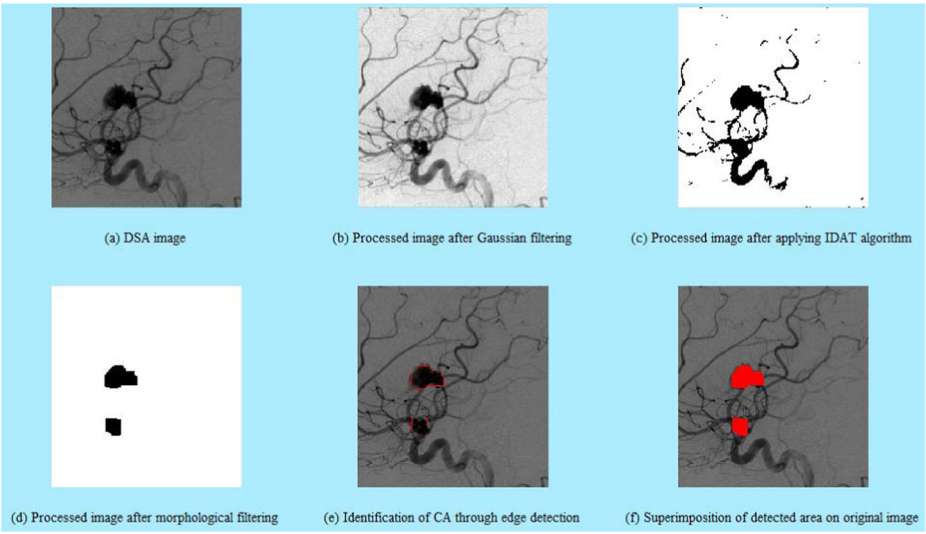

Fig. 20 Detection of CA from test image 14

forms the backbone of our contribution. Upper and lower threshold values of this algorithm have been selected in an iterative way. Supremacy of the proposed IDAT algorithm over other existing thresholding algorithms like Otsu's threshold, Sauvola's threshold and Niblack's threshold has been established with the aid of a number of test images. It has been shown that single and multiple cerebral aneurysms can be successfully detected by means of our proposed algorithm. Moreover, automated thresholding algorithm together with the morphological filtering becomes successful to identify the aneurysm portion only without human

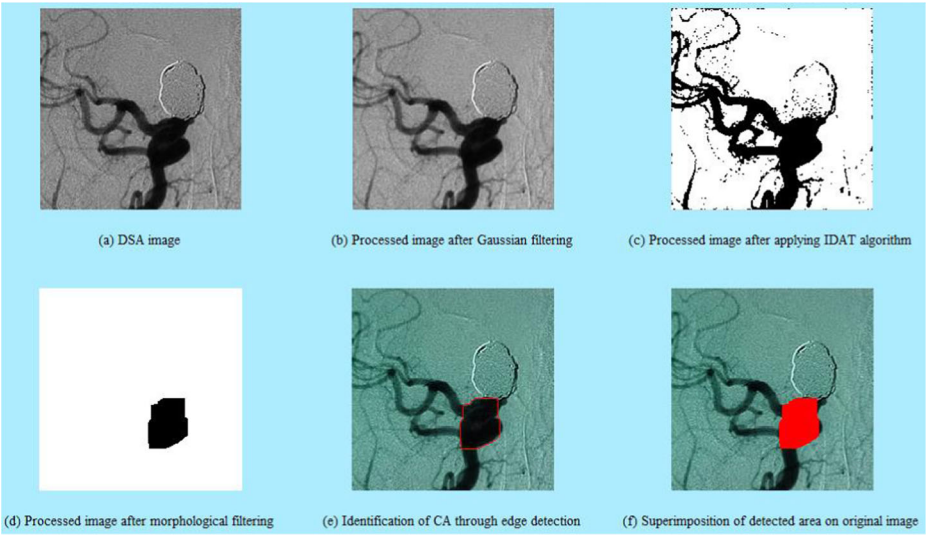

Fig. 21 Detection of CA from test image 15

Table 2 Comparative analysis with other state-of-the-art techniques for the detection of CA

Algorithm		Accuracy (%)	Sensitivity	Specificity	Type of the image
J. P. Villablanca et al. [31]		99.5	0.99	1	DSA
A. McKinney et al. [15]		95.8	0.97	0.9	Multisection CT Angiography
M. Li et al. [13]		99.3	0.98	1	DSA
J. Mitra et al. [19]		96.9	1	1	DSA
Proposed Algorithm	Test image 1	99.65	1	1	DSA
	Test image 2	99.98	1	1	
	Test image 3	98.82	0.96	1	
	Test image 4	99.73	1	1	
	Test image 5	99.17	0.98	1	
	Test image 6	99.94	0.98	1	
	Test image 7	99.86	0.99	1	
	Test image 8	97.47	0.95	1	
	Test image 9	98.63	0.97	1	
	Test image 10	96.12	0.96	0.9	
	Test image 11	98.89	1	1	
	Test image 12	98.71	0.97	1	
	Test image 13	99.26	1	1	
	Test image 14	98.15	0.98	0.95	
	Test image 15	99.03	0.99	1	
Average performance of all the images resulting from the proposed algorithm		98.894	0.982	0.99	

intervention and eliminates the gratuitous blood vessels from the DSA images. A set of fifteen test images has been selected for the purpose of demonstrating our observation. Supremacy of our proposition has been ascertained by means of relevant performance indices both qualitatively and quantitatively. Future research may be carried out in the direction of finding out proper correlation between the size and multiplicity of aneurysm with the accuracy, sensitivity and specificity of detection.

References

1. Basak K, Patra R, Manjunatha M, Dutta PK (2012) Automated detection of air embolism in OCT contrast imaging: anisotropic diffusion and active contour based approach. 3rd International Conferene on Emerging Applications of Information Technology (EAIT), pp 110–115
2. Bhadri PR, Kumar AS, Salgaonkar VA, Kumar G, Beyette FR Jr, Clark JF (2005) Development of an integrated hardware and software platform for the rapid detection of cerebral aneurysm, in 48th Midwest symposium on circuits and systems. IEEE 2:1924–1927. doi:10.1109/MWSCAS.2005.1594502
3. Bisbal J, Engelbrecht G, Villa-Uriol M-C, Frangi AF (2011) Prediction of cerebral aneurysm rupture using hemodynamic, morphologic and clinical features: a data mining approach. In: Database and expert systems applications. Springer, pp 59–73
4. Brady AR, Thompson S (2002) Making predictions from hierarchical models for complex longitudinal data, with application to aneurysm growth. MRC Biostatistics Unit, Cambridge, pp 1–25

5. Brain aneurysms foundations, cerebral aneurysm resources. Available: http://bafoundations.com/ImageGallery.html, 2013
6. Cárdenes R, Pozo JM, Bogunovic H, Larrabide I, Frangi AF (2011) Automatic aneurysm neck detection using surface voronoi diagrams. IEEE Transactions on Medical Imaging 30(10):1863–1876. doi:10.1109/TMI.2011.2157698
7. Cebral JR, Castro MA, Appanaboyina S, Putman CM, Millan D, Frangi AF (2005) Efficient pipeline for image-based patient-specific analysis of cerebral aneurysm hemodynamics: technique and sensitivity. IEEE Trans Med Imaging 24(4):457–467. doi:10.1109/TMI.2005.844159
8. Dr. Balaji Anvekar's neuroradiology cases, Neuroradiology cases. Available: http://www.yousaytoo.com/aneurysm-dsa/1896957
9. Farnoush A, Qian Y, Takao H, Murayama Y, Avolio A (2012) Effect of saccular aneurysm and parent artery morphology on hemodynamics of cerebral bifurcation aneurysms. In: 34th annual international conference of the IEEE engineering in medicine and biology society (EMBC). IEEE, San Diego, pp. 6677–6680
10. Hentschke CM, Beuing O, Nickl R, Tonnies KD (2011) Automatic cerebral aneurysm detection in multimodal angiographic images. Nuclear Science Symposium and Medical Imaging Conference (NSS/MIC), 2011 IEEE, pp 3116–3120. doi:10.1109/NSSMIC.2011.6152566
11. Hentschke CM, Tonnies K, Beuing O, Nickl R (2012) A new feature for automatic aneurysm detection, 9th IEEE international symposium on biomedical imaging (ISBI). IEEE, Barcelona, Spain, pp. 800–803. doi:10.1109/ISBI.2012. 6235669
12. Kroon M (2011) Simulation of cerebral aneurysm growth and prediction of evolving rupture risk. Model Simul Eng 2011:3. doi:10.1155/2011/289523
13. Li M, Cheng Y, Li Y, Fang C, Chen S, Wang HD, Xu H (2009) Large-cohort comparison between three-dimensional time-of-flight magnetic resonance and rotational digital subtraction angiographies in intracranial aneurysm detection. Stroke 40(9):3127–3129
14. Loong T (2003) Understanding sensitivity and specificity with the right side of the brain. BMJ: Br Med J 327(7417):716
15. McKinney A, Palmer C, Truwit C, Karagulle A, Teksam M (2008) Detection of aneurysms by 64-section multidetector CT angiography in patients acutely suspected of having an intracranial aneurysm and comparison with digital subtraction and 3D rotational angiography. Am J Neuroradiol 29(3):594–602
16. Meng H, Wang Z, Hoi Y, Gao L, Metaxa E, Swartz DD, Kolega J (2007) Complex hemodynamics at the apex of an arterial bifurcation induces vascular remodeling resembling cerebral aneurysm initiation. Stroke 38(6):1924–1931. doi:10.1161/STROKEAHA.106.481234
17. Mikhal J, Lopez Penha DJ, Slump CH, Geurts BJ (2010) Immersed boundary method predictions of shear stresses for different flow topologies occuring in cerebral aneurysms, European conference on computational fluid dynamics. ECCOMAS, Lisbon
18. Mitra J, Chandra A (2013) Detection of cerebral aneurysm by performing thresholding-spatial filtering-thresholding operations on digital subtraction angiogram. Advances in computing and information technology. Springer, Berlin Heidelberg, pp 915–921. doi:10.1007/978-3-642-31552-7_93
19. Mitra J, Chandra A, Halder T (2013) Peak trekking of hierarchy mountain for the detection of cerebral aneurysm using modified hough circle transform. Electron Lett Comput Vis Image Anal 12(1):57–84
20. Niblack W (1986) An introduction to image processing. Prentice-Hall, Englewood Cliffs, NJ, pp. 115–116
21. Nikravanshalmani A, Qanadli SD, Ellis TJ, Crocker M, Ebrahimdoost Y, Karamimohammdi M, Dehmeshki J (2010) Three-dimensional semi-automatic segmentation of intracranial aneurysms in CTA, 10th IEEE international conference on information technology and applications in biomedicine (ITAB). IEEE, Corfu, pp. 1–4. doi:10.1109/ITAB.2010.5687759
22. Otsu N (1975) A threshold selection method from gray-level histograms. Automatica 11(285–296):23–27
23. Piccinelli M, Veneziani A, Steinman DA, Remuzzi A, Antiga L (2009) A framework for geometric analysis of vascular structures: application to cerebral aneurysms. IEEE Trans Med Imaging 28(8):1141–1155. doi:10.1109/TMI.2009.2021652
24. Rahman M, Smietana J, Hauck E, Hoh B, Hopkins N, Siddiqui A, Levy EI, Meng H, Mocco J (2010) Size ratio correlates with intracranial aneurysm rupture status a prospective study. Stroke 41(5):916–920. doi:10.1161/STROKEAHA.109.574244
25. Sauvola J, Pietikainen M (2000) Adaptive document image binarization. Pattern Recogn 33(2):225–236
26. Shimogonya Y, Itoh K, Kumamaru H (2010) Computational simulation of blood flow dynamics using an anatomically realistic artery model constructed from medical images, World Automation Congress (WAC), IEEE, Kobe: TSI Press, pp 1–5, ISBN:978–1–4244–9673-0
27. Uchiyama Y, Yamauchi M, Ando H, Yokoyama R, Hara T, Fujita H, Iwama T, Hoshi H (2006) Automated classification of cerebral arteries in MRA images and its application to maximum intensity projection, 28th annual international conference of the IEEE engineering in medicine and biology society, EMBS'06. IEEE, New York, pp. 4865–4868. doi:10.1109/IEMBS.2006.260438

28. Ujiie H, Tamano Y, Sasaki K, Hori T (2001) Is the aspect ratio a reliable index for predicting the rupture of a saccular aneurysm? Neurosurgery 48(3):495–503
29. Utami N, Zakaria H, Mengko TL, Santoso OS (2011) Role of pressure and wall shear stress in initiation and development of cerebral aneurysms, 2nd international conference on instrumentation, communications, information technology, and biomedical engineering (ICICI-BME). IEEE, Bandung, pp. 310–314. doi:10.1109/ICICI-BME.2011.6108629
30. Valencia C, Villa-Uriol M, Pozo J, Frangi A (2010) Morphological descriptors as rupture indicators in middle cerebral artery aneurysms, 32nd annual international conference of the IEEE engineering in medicine and biology society (EMBC). IEEE, Buenos Aires, pp. 6046–6049
31. Villablanca JP, Jahan R, Hooshi P, Lim S, Duckwiler G, Patel A, Sayre J, Martin N, Frazee J, Bentson J et al (2002) Detection and characterization of very small cerebral aneurysms by using 2D and 3D helical CT angiography. Am J Neuroradiol 23(7):1187–1198
32. Wang Y, Courbebaisse G, Zhu YM (2011) Segmentation of giant cerebral aneurysms using a multilevel object detection scheme based on lattice Boltzmann method, international conference on signal processing, communications and computing (ICSPCC). IEEE, Xi'an, pp. 1–4. doi:10.1109/ICSPCC.2011.6061695
33. Wardlaw JM, White PM (2000) The detection and management of unruptured intracranial aneurysms. Brain 123(2):205–221. doi:10.1093/brain/123.2.205
34. Wermer MJ, Van der Schaaf IC, Algra A, Rinkel GJ (2007) Risk of rupture of unruptured intracranial aneurysms in relation to patient and aneurysm characteristics an updated meta-analysis. Stroke 38(4):1404–1410. doi:10.1161/01.STR.0000260955.51401.cd
35. Wiebers DO (2003) Unruptured intracranial aneurysms: natural history, clinical outcome, and risks of surgical and endovascular treatment. Lancet 362(9378):103–110
36. Wu J, Zhang G, Cao Y, Cui Z (2009) Research on cerebral aneurysm image recognition method using bayesian classification, 2009 international symposium on information processing (ISSP'09), pp. 58–62
37. Zakaria H, Kurniawan A, Mengko TLR, Santoso OS (2011) Detection of cerebral aneurysms by using time based parametric color coded of cerebral angiogram. International Conference on Electrical Engineering and Informatics, Bandung. doi:10.1109/ICEEI.2011.6021503
38. Zubillaga AF, Guglielmi G, Viñuela F, Duckwiler GR (1994) Endovascular occlusion of intracranial aneurysms with electricallly detachable coils: correlation of aneurysm neck size and treatment results. AJNR Am J Neuroradiol 15(5):815–820

Abhijit Chandra (abhijit922@yahoo.co.in) has obtained B. E. in Electronics & Telecommunication Engineering from Indian Institute of Engineering Science and Technology, Shibpur (Formerly, Bengal Engineering & Science University, Shibpur), India in 2008 and M. E. Tel. E with specialization in Communication Engineering and Ph. D (Engineering) from Jadavpur University, India in 2010 and 2016 respectively. He was associated with the Department of Electronics & Telecommunication Engineering, Indian Institute of Engineering Science and Technology, Shibpur as Assistant Professor from 2010 to 2014. Presently, he is working as an Assistant Professor in the Department of Instrumentation & Electronics Engineering, Jadavpur University. His research area includes Digital Signal/Image Processing, Evolutionary Optimization Techniques, Digital/Mobile Communication Systems, Information and Coding Theory. He has published more than 40 research papers in International/National Conferences and Journals of good repute. He has also been working as a guest reviewer of many internationally acclaimed journals like International Journal of Electronics (Taylor & Francis), Circuits, Systems, and Signal Processing (Springer) etc. He has carried out the responsibility of workshop coordinator for NMEICT workshop

on Signals & Systems jointly organized by IIT Bombay and IIT Kharagpur in 2014. Dr. Chandra has received President's Gold Medal from Bengal Engineering & Science University, Shibpur in 2010 for being First in the faculty of Engineering and Technology at B. E. examination 2008. He has also received University Medal in 2010 for standing First in order of merit at the M. E. Tel. E. examination 2010 from Jadavpur University. He has received Plaque from Texas Instruments for guiding one student project successfully in TI India Analog Design Contest 2011. The project was among the Top-15 projects among the 156 entries submitted to the contest. Dr. Chandra has very recently received "IEI Young Engineers Award 2015-2016" in Electronics & Telecommunication Engineering discipline from the Institution of Engineers (India) in recognition of his achievement in engineering research.

Sumita Mondal (sumitam95@gmail.com) has received her B. Tech in Electronics and Communication Engineering from Jalpaiguri Government Engineering College, India and M. E. in Electronics and Telecommunication Engineering with specialization in Communication Engineering and Signal Processing from Indian Institute of Engineering Science and Technology, Shibpur. Presently, she is pursuing Ph.D. from School of Medical Science & Technology, Indian Institute of Technology, Kharagpur. Her research area includes biomedical image processing.